Analytica Chimica Acta xxx (xxxx) xxx

Contents lists available at ScienceDirect

Analytica Chimica Acta

journal homepage: www.elsevier.com/locate/aca

Label-free peptide nucleic acid biosensor for visual detection of multiple strains of influenza A virus suitable for field applications

Naveen Kumar [a, *], Sandeep Bhatia [a], Atul Kumar Pateriya [a], Richa Sood [a], S. Nagarajan [b], Harshad V. Murugkar [b], Satish Kumar [c, 1], Praveen Singh [c, d], Vijendra Pal Singh [a]

[a] Diagnostics & Vaccines Section, ICAR-National Institute of High Security Animal Diseases, Bhopal, 462022, India
[b] Avian Diseases Section, ICAR-National Institute of High Security Animal Diseases, Bhopal, 462022, India
[c] Central Instrumentation Facility- Bioengineering, ICAR-Indian Veterinary Research Institute, Izatnagar, Bareilly, 243122, India
[d] Biophysics and Electron Microscopy Section, ICAR-Indian Veterinary Research Institute, Izatnagar, Bareilly, 243122, India

HIGHLIGHTS

- A rapid and label-free visual assay for multiple strains of Influenza A Virus.
- The method provides accurate quantification of viral RNA on a spectrophotometer.
- The assay shows high diagnostic sensitivity and specificity on clinical samples.
- Offers new prospects for rapid point-of-care diagnostics against many pathogens.

GRAPHICAL ABSTRACT

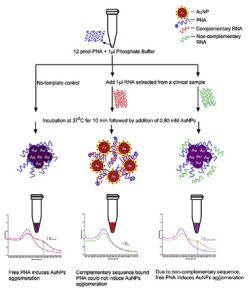

ARTICLE INFO

Article history:
Received 21 August 2019
Received in revised form
21 September 2019
Accepted 23 September 2019
Available online xxx

Keywords:
Label-free visual assay
Influenza A viruses
Peptide nucleic acid
Gold nanoparticles

ABSTRACT

Accurate and rapid diagnosis of Influenza A viruses (IAVs) is challenging because of multiple strains circulating in humans and animal populations, and the emergence of new strains. In this study, we demonstrate a simple and rapid strategy for visual detection of multiple strains of IAVs (H1 to H16 subtypes) using peptide nucleic acid (PNA) as a biosensor and unmodified gold nanoparticles (AuNPs) as a reporter. The design principle of the assay is based on the color change on account of free PNA-induced aggregation of AuNPs in the presence of non-complementary viral RNA sequence and *vice-versa*. The assay could detect IAV RNA with a visual limit of detection of 2.3 ng. The quantification of RNA with a considerable accuracy on a simple spectrophotometer was achieved on plotting the PNA-induced colorimetric changes (absorption ratio of A_{640}/A_{520}) in the presence of a varying concentration of complementary RNA. As a proof-of-concept, the visual assay was validated on 419 avian clinical samples and receiver operating characteristic (ROC) curve analysis showed a high diagnostic specificity (96.46%, 95% CI = 93.8 to 98.2) and sensitivity (82.41%, 95% CI = 73.9 to 89.1) when RT-qPCR was used as reference test. Hence, the simplicity, rapidity, and universality of this strategy make it a potential candidate visual assay for clinical diagnosis and surveillance of IAVs, especially in the resource-limited settings. The proposed strategy establishes new avenues for developing a simple and rapid diagnostic system for viral infections and biomolecules.

© 2019 Elsevier B.V. All rights reserved.

* Corresponding author.
E-mail addresses: navyog.yadav84@gmail.com, naveen.kumar4@icar.gov.in (N. Kumar).
[1] Present address: 1643P, Sector-9A, Bahadurgarh 124507, Haryana, India.

https://doi.org/10.1016/j.aca.2019.09.060
0003-2670/© 2019 Elsevier B.V. All rights reserved.

Please cite this article as: N. Kumar et al., Label-free peptide nucleic acid biosensor for visual detection of multiple strains of influenza A virus suitable for field applications, Analytica Chimica Acta, https://doi.org/10.1016/j.aca.2019.09.060

1. Introduction

Influenza A viruses (IAVs) being accountable for several epizootics pose a continuous worldwide threat to the poultry industry and public health. The avian species within the orders *Anseriformes* and *Charadriiformes* serve as natural reservoirs for IAVs [1]. Based on the antigenic differences in their surface glycoproteins, IAVs have been classified into 18 HA (H1–H18) and 11 NA (N1–N11) subtypes. Some 122 million domestic birds have been wiped out due to H5N1 outbreaks in the last five years and more than half (58%) cases were from Asia alone [2]. As of April 2019, 860 cases of zoonotic human infections with H5N1 have been reported from 16 countries, of which 454 were fatal [3]. The diagnosis of IAVs is being carried out regularly by virus isolation, conventional RT–PCR, and real-time quantitative RT–PCR (RT–qPCR). The virus isolation is time-consuming and prone to false-negative results. Both RT–PCR and RT–qPCR are highly sensitive and specific for detection of IAVs, however, the requirement of sophisticated instrumentation, skilled personnel, and poor stability of reagents prohibits their use as a field diagnostic test. The microfluidics chip-based devices have therefore been explored to overcome some of these limitations, however, expensive instrumentation and sophisticated fabrication protocols limit their use in resource-limited settings [4,5]. Even though commercial rapid influenza diagnostic tests (RIDTs) can overcome these limitations, their high cost and frequent inaccuracies render them an unsuitable diagnostic candidate for large-scale adoption [6]. The World Health Organization (WHO) has developed the ASSURED (Affordable, Sensitive, Specific, User-friendly, Rapid and robust, Equipment-free and Deliverable to end-users) criteria to select an appropriate diagnostic test that can be used in resource-limited settings effectively. Thus, diagnostic methods that conform to the WHO ASSURED criteria could play a decisive role not only to control the rapid spread of IAVs during an outbreak but also for reducing the economic burden on the poultry industry and mitigating the associated public health risks [7].

The colorimetric assays based on accruement of metallic nanoparticles have received substantial attention in the rapid diagnostic field due to their cost-effectiveness, high sensitivity, simplicity, and no requirement of sophisticated instrumentation [8]. Among the metallic nanoparticles, gold nanoparticles (AuNPs) offer many superior qualities that earn them an ideal and promising candidate in the development of cost-effective rapid diagnostic assays. These include ease of synthesis in the laboratory, non-interference with other labeled biomaterials, high chemical stability and ability to interact with nucleic acids, aptamers and peptide nucleic acids (PNAs). The covalent conjugation of the nucleotides or aptamers or PNA probes onto AuNPs has been used frequently for the detection of biomolecules or chemicals such as analyte [9], mRNA [10], DNA [11], RNA [12], microRNA [13] and biomarker [14]. However, conjugation of probes with AuNPs is time-consuming and involves tedious procedures. Thus, it would be an ideal strategy to develop methods that do not require such conjugation procedures.

PNAs offer several advantages over nucleic acid oligomers such as stable duplex structures with complementary DNA or RNA sequences, high thermal stability and resistance to degradation by nucleases and proteases, and extreme stability in acidic environments [15,16]. The ability of charge-neutral PNA to induce immediate aggregation of AuNPs can be used for the development of a label-free visual assay [17,18]. In this paper, we report the development of a label-free rapid visual assay for the detection and quantification of IAV RNA based on the inhibition of free PNA induced aggregation of AuNPs in the presence of complementary RNA sequence and *vice-versa*. The analytical specificity of the visual assay was determined against diverse IAVs HA subtypes. Furthermore, we evaluated the diagnostic performance of the visual assay on 419 avian clinical samples and the results were compared with RT–qPCR, which is a standard diagnostic assay for IAVs.

2. Materials and methods

2.1. Reagents and chemicals

The Fmoc-PNA monomers and linker, [2-(2-(Fmoc-amino) ethoxy)ethoxy]acetic acid (AEEA) were purchased from Panagene Inc. (South Korea). Rink amide-MBHA resin (100–200 mesh, 0.30 mM/g of the resin) was procured from Merck (China) while pyridine, m-cresol, triisopropyl silane (TIS), especially dried N, N-dimethylformamide (DMF), dichloromethane (DCM), methanol, piperidine, diethyl ether, and HPLC-grade water were from Merck (Germany). The Gold(III) chloride trihydrate ($HAuCl_4 \cdot 3H_2O$), 1-[Bis(dimethylamino)methylene]-1H-1,2,3-triazolo[4,5-b]pyridinium 3-oxide hexafluorophosphate (HATU) and N,N-Diisopropylethylamine (DIEA) were procured from Sigma–Aldrich (Germany). Oligonucleotides were custom synthesized, and the chemicals and reagents were of analytical grade (unless specified otherwise).

2.2. Instrumentation

The designed PNA was synthesized on an Aapptec Labmate 4 × 6 peptide synthesizing platform. The PNA was desalted and purified by Reverse-Phase High-Performance Liquid Chromatography (RP-HPLC) on a Shimadzu LC20 ADHPLC (Japan). The transmission electron microscopy (TEM) measurements of AuNPs were made on a TALOS 200 kV S-FEG (FEI, USA) which is a FIST supported TEM facility at Department of Chemistry, Indian Institute of Science Education and Research (IISER), Bhopal, India on an accelerating voltage of 200 kV. The zeta potential measurements of AuNPs were built on a Beckman Coulter Delsa™ Nano (USA) at Department of Chemistry, IISER, Bhopal, India. The intact mass analysis of PNA was done on a MALDI Ultraflex–TOF–TOF mass spectrometer by Sandor Lifesciences Pvt. Ltd., India. The absorbance spectra were recorded on a Spectra-Max M5 (Molecular Devices, USA) using quartz cuvettes with an optical path length of 1 cm at room temperature. Real-time PCR experiments were performed on a Light Cycler® 480 II Real-Time PCR (Roche, Germany).

2.3. Sampling of clinical cases

A total of 419 cloacal samples representing avian species from two distinct geographical locations (n = 325) in India, including IAV confirmed positive (n = 50) and negative (n = 44) samples received from the Avian Influenza repository of the National Institute of High Security Animal Diseases, Bhopal, India were used in this study (Table S1). The avian species-wise samples distribution is as follows; Duck (n = 10), Goose (n = 3), Kite (n = 4), Pigeon (n = 43), Quail (n = 4), Turkey (n = 6), Crane (n = 1), SPF Chicken (n = 44), Chicken (n = 297), Cockatoo (n = 2) and Pheasant (n = 5). All the samples were processed for viral RNA extraction and tested for IAVs using the PNA visual assay and the RT–qPCR.

2.3.1. RT–qPCR

Viral RNA from the respective clinical samples was extracted using NucleoSpin RNA Virus, MACHEREY-NAGEL GmbH & Co. KG (TaKaRa, Japan) as per the recommendations of the manufacturer. One-step RT-qPCR was carried out in duplicates using GoTaq Probe 1-step RT-qPCR system (Promega, USA) in a total volume of 12.5 μL containing 6.25 μL 2X buffer, 0.5 μL of 20 pmol each forward (5′-TGATCTTCTTGAAAATTTGCAG-3′) and reverse (5′-CCGTAG-MAGGCCCTCTTTTCA-3′) primers, 0.25 μL of 10 pmol probe (FAM-

Please cite this article as: N. Kumar et al., Label-free peptide nucleic acid biosensor for visual detection of multiple strains of influenza A virus suitable for field applications, Analytica Chimica Acta, https://doi.org/10.1016/j.aca.2019.09.060

TTGTGGATTCTTGATCG-BHQ-1), 0.25 μL of 50X GoScript™ RT mix, 3.75 μL of nuclease-free water and 1 μL of viral RNA. The thermal profile was programmed as 30 min at 50 °C for reverse transcription, 2 min at 95 °C for initial denaturation followed by 40 cycles of a 3 step PCR, including 95 °C for 30 s, 50 °C for 1 min and 72 °C for 30 s. No template control and no probe control were included in each run.

2.4. Designing, synthesis and characterization of PNA

The complete coding nucleotide sequences of matrix (M) gene of Influenza A viruses (n = 42372) were retrieved from the NCBI database (https://www.ncbi.nlm.nih.gov/genomes/FLU/Database/nph-select.cgi?go=database, accessed on November 1, 2016) and generated HA-subtype specific consensus sequences using multiple sequence alignment by MAFFT version 7.222. The numbers of HA-subtype specific M gene sequences used to generate consensus sequences are provided in Table S2. These consensus sequences were further aligned to design a highly conserved target region within the M gene that constituted a 16-mer poly-pyrimidine rich tract for the laboratory synthesis of PNA (Fig. 1A and B). The nucleotide composition analysis of the designed PNA is given in Table S3.

The designed PNA was synthesized in the laboratory by solid-phase peptide synthesis employing Fmoc chemistry on Rink Amide-MBHA resin [19]. Briefly, a Rink Amide-MBHA resin LL (20 mg, 0.30 mM/g) was swelled in DMF overnight followed by removal of resin-bound Fmoc protecting group by treating with 20% (v/v) piperidine solution in DMF. The first amide coupling was carried out by mixing 5 M equiv (as per the initial loading of the resin) of AEEA in DMF, HATU (4.5 M equiv) in DMF, DIEA (10 M equiv), and Pyridine (2.5 M equiv) for 10 min and this solution mixture was added over the pre-swollen resin. The mixture was shaken at room temperature (22–25 °C) in a shaker-cum-incubator for 2 h at 120 rpm and then washed with DMF (3 × 1 min), DCM (3 × 1 min) and DMF (3 × 1 min). The remaining free amines were capped by treating with 0.5 mL of acetylating solution (DMF, Acetic anhydride, and DIEA in the ratio of 89:5:6, v/v) for 10 min with gentle shaking. Subsequently, the elongation of PNA sequence was obtained by repeated cycles of Fmoc deprotection by 20% (v/v) piperidine solution in DMF and coupling reactions as described above. Every step of deprotection and coupling during the elongation of PNA sequence was monitored by Kaiser (ninhydrin) test. Once the desired PNA length was achieved, the bound PNA was cleaved from the resin by treating with 0.5 mL of cleavage mixture (TFA, Phenol, Thioanisol, Ether and HPLC Water in the ratio of 85:10:2.5:2.5, v/v) for 5 h at room temperature (22–25 °C) with gentle shaking. The cleaved PNA was then precipitated by chilled diethyl ether and dissolved in HPLC-grade water. The PNA was purified and desalted by RP-HPLC (solvent A: HPLC-grade water + 0.1% TFA; solvent B: acetonitrile + 0.1% TFA; from 5 to 70% of solvent B over 40 min, increment rate: 1% acetonitrile/min, flow rate: 0.8 mL/min). The fraction of interest was manually collected, vacuum dried, and dissolved in HPLC-grade water. The molecular weight of PNA was analyzed by MALDI Ultraflex–TOF–TOF while the concentration was measured on Eppendorf Bio-spectrophotometer at 260 nm.

2.5. Synthesis and characterization of colloidal gold

All the glassware was treated with freshly prepared aqua-regia (one part of nitric acid and 3 parts of hydrochloric acid), rinsed thoroughly with double distilled water and oven-dried before use. The citrate stabilized gold nanoparticles (AuNPs) were synthesized by reduction of Gold (III) chloride trihydrate ($HAuCl_4 \cdot 3H_2O$) by sodium citrate [20]. Briefly, 100 mL of 1 mM $HAuCl_4 \cdot 3H_2O$ solution was boiled for 5 min with vigorous stirring on a hot plate magnetic stirrer and then pre-boiled 10 mL of 38.8 mM trisodium citrate solution was rapidly added. The solution was boiled with vigorous stirring for another 10 min, during which time its color changed from pale-yellow to brick red-wine. The solution was then cooled to room temperature with continuous stirring. The resulting brick red-wine solution was stored at 4 °C until further use. The AuNPs were characterized for their typical absorbance at 520 nm in a UV–vis spectrophotometer. Furthermore, the shape and size of the AuNPs were analyzed by TEM and dynamic light scattering (DLS).

2.6. Colorimetric procedure for the visual assay

To develop an optimized protocol for the visual detection of IAV RNA, the concentration of PNA required for complete aggregation of 0.80 mM AuNPs was determined by reacting varying concentrations of PNA to AuNPs and recorded the absorption spectra from 400 to 750 nm wavelength on a Spectra-Max M5 (Molecular Devices, USA). Subsequently, absorption spectra of fixed PNA concentration reactivity with 2-fold serial dilutions of complementary oligo were recorded. To detect an IAV specific RNA sequence, 12 pmol of PNA was mixed with 1 μL RNA sample in the presence of 1 μL of 10 mM Phosphate Buffer (pH 7.2) solution containing 0.1 mM EDTA and 150 mM NaCl and incubated at 37 °C for 10 min. 10 μL of 0.80 mM AuNPs was then added to a PNA-RNA mixture solution and kept for 1 min at room temperature. To improve the color discrimination, 1 μL of 10 mM Phosphate Buffer was added. A change in color from red to purple/blue was recorded visually and also analyzed on a spectrophotometer. The optimized visual assay was then used to detect and quantify the IAV RNA in the avian cloacal samples. The specificity of the IAVs RNA detection was monitored in the presence of the negative and blank controls that contained RNA extracted from a cloacal sample of an Influenza-free chicken (specific pathogen-free chicken) and HPLC grade water, respectively.

2.7. Data analysis

The receiver operating characteristic (ROC) curve analysis was performed by MedCalc® statistical software version 19 where true IAV positive and negative samples were assigned the values of 1 and 0, respectively. The area under the ROC curve (AUC) was then calculated for the samples tested by different diagnostics assays [21]. Furthermore, inter-rater reliability analysis using the Kappa (κ) statistic to assess the concordance between the diagnostic assays was estimated [22]. All the graphs were generated by GraphPad Prism 8 (GraphPad Software, San Diego, California, USA).

3. Results and discussion

3.1. Design principle and development process of visual IAV RNA detection

3.1.1. Concept

The basic idea of using PNA probe and unmodified AuNPs to develop a label-free visual assay for the detection of viral RNA is based on the fact that charge-neutral PNA causes immediate aggregation of the citrate anions-protected AuNPs that leads to change in color from red to blue/purple. The immediate aggregation of AuNPs occurs because of the distinct backbone properties of PNA (neutrality, high rigidity, and peptide composition). The neutrality allows the PNA to coat and shield negatively charged citrate anions-protected AuNPs, abolishing charge repulsion among

Please cite this article as: N. Kumar et al., Label-free peptide nucleic acid biosensor for visual detection of multiple strains of influenza A virus suitable for field applications, Analytica Chimica Acta, https://doi.org/10.1016/j.aca.2019.09.060

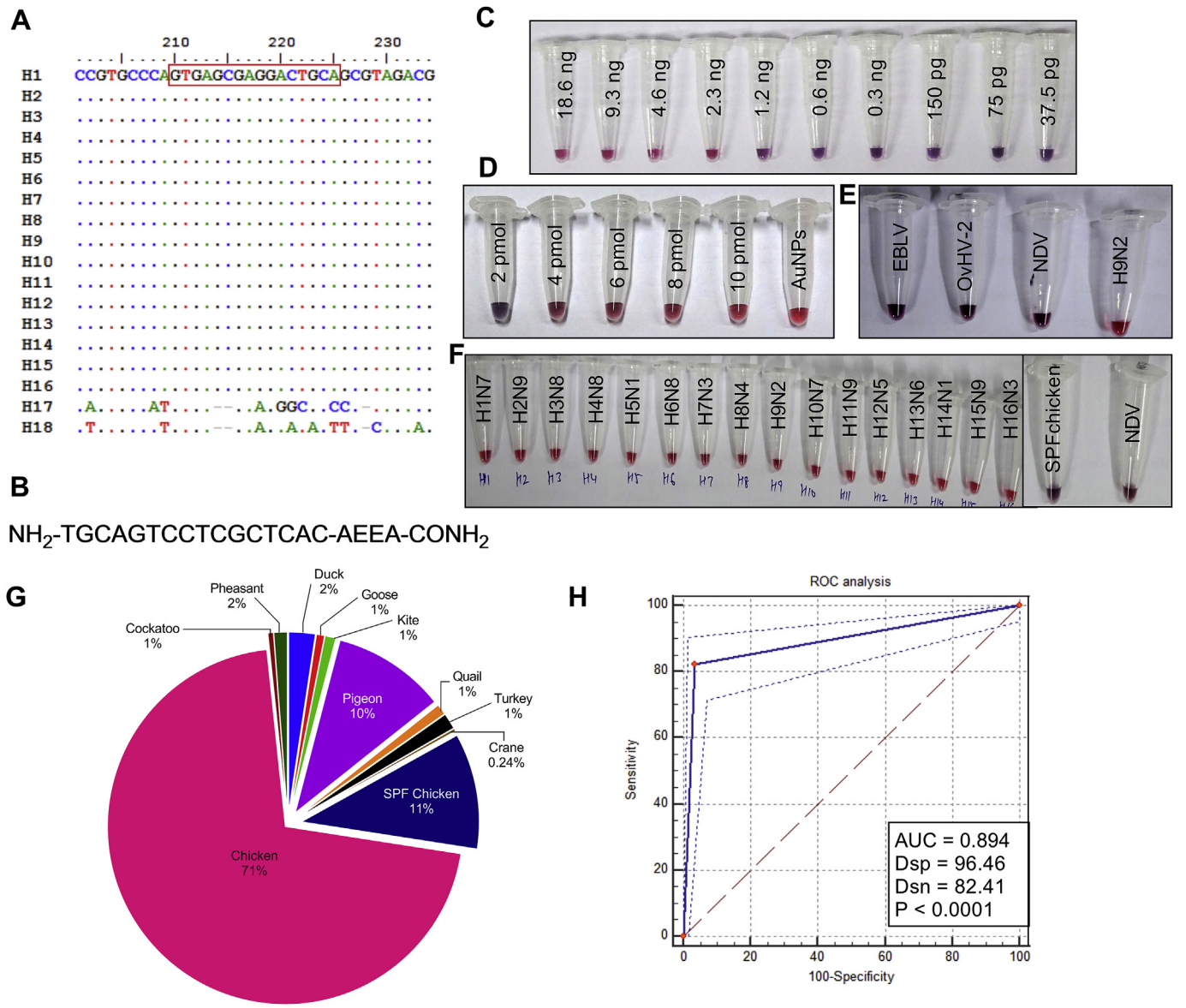

Fig. 1. (A) Multiple sequence alignment of complete coding sequences of matrix gene of IAVs; (B) A 16-mer poly-pyrimidine rich peptide nucleic acid biosensor sequence designed for laboratory synthesis; Visual detection limit of the assay for the detection of (C) IAV RNA (2.3 ng) and (D) $oligo_{comp}$ (4 pmol); (E) Reactivity of PNA with closely (NDV) and distantly related (EBLV and OvHV-2) viruses, (F) Analytical specificity of the visual assay shows 100% specific reactivity (no change in color) to all IAV H1−H16 subtypes, (G) Avian species-wise distribution of clinical samples used in this study, (H) The ROC curve analysis shows a high differentiating power of the assay (AUC = 0.894, 95% CI = 0.861 to 0.922, $p < 0.0001$) with a high diagnostic specificity (96.46, 95% CI = 93.8 to 98.2) and sensitivity (82.41, 95% CI = 73.9 to 89.1). (For interpretation of the references to color in this figure legend, the reader is referred to the Web version of this article.)

AuNPs. The high rigidity of PNA further allows the nucleobases to shield the citrate anions-protected AuNPs efficiently and finally, the peptide backbone makes secondary interactions with AuNPs [23,24].

Nevertheless, PNA in the presence of RNA_{comp} forms PNA-RNA_{comp} complex, and thus colloidal AuNPs remain stable with no change in color due to non-availability of free PNA (Scheme 1). While in the presence of RNA_{nc}, there is no hybridization of PNA with RNA_{nc}, and therefore free PNA molecules induce immediate aggregation of AuNPs causing a change in color from red to blue/purple. This concept was utilized to develop a label-free visual assay for the detection and quantification of IAV RNA. Furthermore, the pragmatic use of the visual assay for its deployment at the field conditions was assessed on avian clinical samples.

3.1.2. Characterization of reagents

The MALDI Ultraflex−TOF−TOF analysis of our laboratory synthesized PNA revealed a molecular weight of 4634.3 Da (while the estimated molecular weight was 4410.24 Da) (Fig. S1A). A slightly more molecular weight is because of end-capping after each coupling reaction during laboratory synthesis of PNA. As shown in Figs. S1B and S1C, the TEM analysis confirmed that AuNPs are of uniform size of 16 nm, while DLS showed that they are of 21.2 nm. The dis-concordance AuNPs size measured by TEM and DLS was expected because of different principles used for the size measurement (DLS measures the hydrodynamic diameter in the solvent environment while TEM do it in dried one) [25]. The zeta potential of AuNPs was found to be −30.90 mV indicating a stable colloidal solution (Fig. S1D).

Please cite this article as: N. Kumar et al., Label-free peptide nucleic acid biosensor for visual detection of multiple strains of influenza A virus suitable for field applications, Analytica Chimica Acta, https://doi.org/10.1016/j.aca.2019.09.060

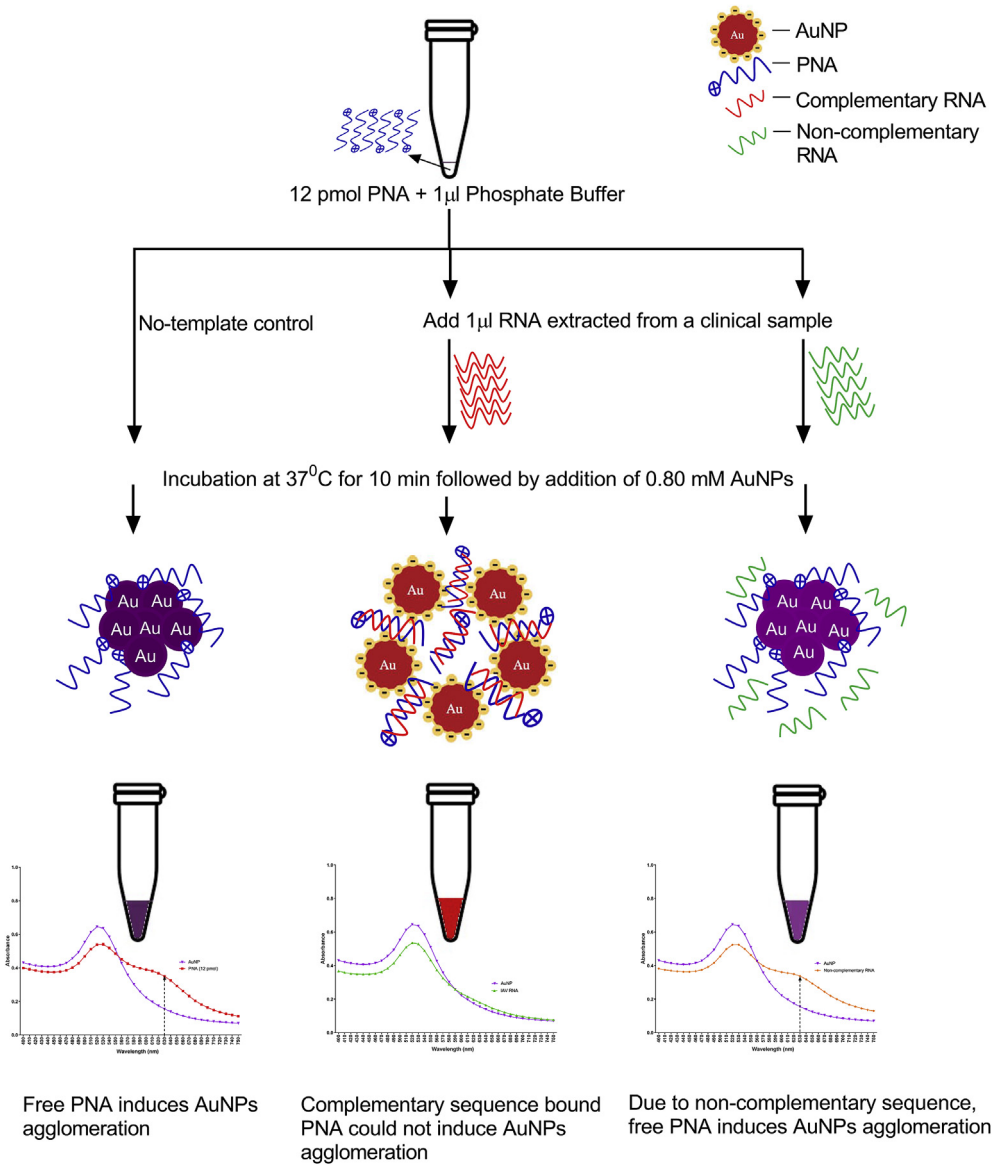

Scheme 1. Schematic illustration of the design principle of the visual assay showing agglomerative behavior of AuNPs in the presence and absence of complementary RNA sequence to PNA.

3.1.3. Development process of a label-free visual assay

We applied the aforementioned concept to develop a label-free visual assay by using a 16−mer PNA sequence designed to target a highly conserved stretch within the M gene of IAV. The PNA concentration required to cause complete aggregation of a fixed amount of AuNPs (10 μL of 0.80 mM) was determined to be 12 pmol and respective absorption spectral changes of different solutions were recorded (Fig. 2A). When an increasing concentration of PNA was added, the well-dispersed AuNPs (red color with a characteristic surface plasmon peak at 520 nm) turned into dark purple, accompanied with a slight shift in the absorption peak to 530 nm and noticeable increasing absorptions at 630 nm (Fig. 2A). For apparent visual changes, 12 pmol of PNA was found sufficient to induce complete aggregation of 10 μL of 0.80 mM AuNPs solution and was used consistently in all other experiments. Similarly, the varying concentrations of $oligo_{comp}$ (2−10 pmol) and IAV RNA (18.6−0.6 ng) were incubated with 12 pmol of PNA separately for 10 min before the addition of AuNPs solution and respective absorption spectra were recorded for each solution (Fig. 2B and C). The colorimetric changes showed apparent color stability of AuNPs solution up to 4 pmol $oligo_{comp}$ and 2.3 ng IAV RNA, indicative of visual detection limits for them (Fig. 1C and D). Thus, the direct IAV RNA concentration of $\geq$2.3 ng is suitable for correct detection procedure visually (naked eye). However, the spectral detection limit was found to be 1.2 ng of IAV RNA.

The presence of secondary or tertiary structures in the target sequence creates a barrier for efficient hybridization with oligonucleotide probes. In particular, these structures of nucleic acid impose substantial thermodynamic penalties and slower kinetics to hybridization with oligonucleotide probes as compared to the denatured or unstructured target sequence. Therefore, the denaturation of nucleic acid becomes an essential step to achieve an efficient and specific hybridization to oligonucleotide probes. However, the high-affinity oligonucleotide analogues such as PNA can compensate for the thermodynamic and kinetic barriers to hybridization with the target sequence [26]. The low-salt conditions could furthermore facilitate PNA-RNA hybridization by destabilization of target secondary structure significantly [27]. This

Please cite this article as: N. Kumar et al., Label-free peptide nucleic acid biosensor for visual detection of multiple strains of influenza A virus suitable for field applications, Analytica Chimica Acta, https://doi.org/10.1016/j.aca.2019.09.060

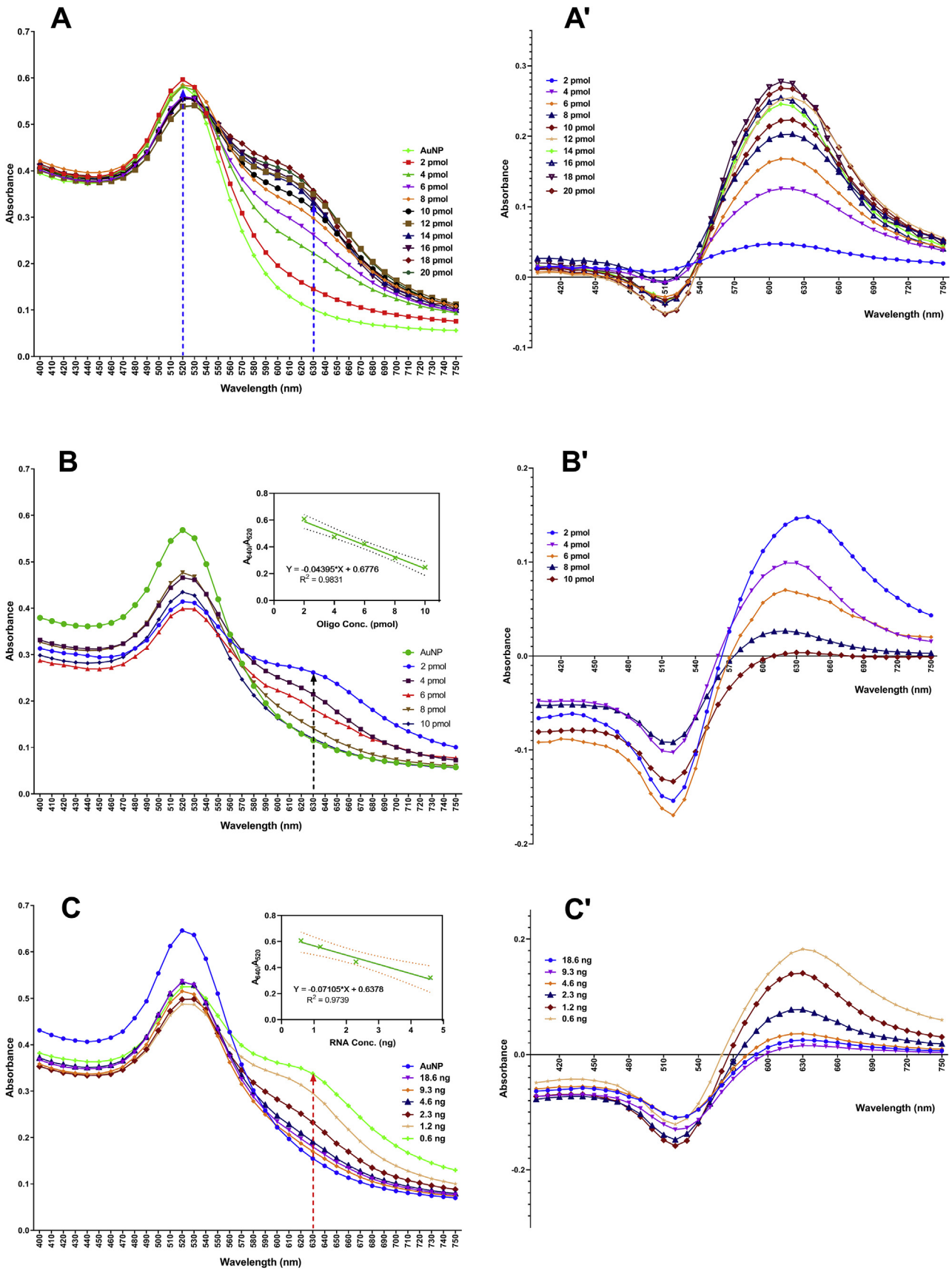

Fig. 2. The concentration-dependent absorption spectra of (A) AuNPs solution incubated with varying PNA concentrations (2–20 pmol); AuNPs solution after incubation of 12 pmol PNA with (B) $oligo_{comp}$ (2–10 pmol) and (C) IAV RNA (0.6–18.6 ng). Also, a plot of OD_{640nm}/OD_{520nm} as a function of $oligo_{comp}$ (B) and IAV RNA (C) concentration shows a linear correlation of $R^2 = 0.983$ and $R^2 = 0.974$, respectively for the quantitative assay. 2A′, B' & C′ depict the concentration-dependent spectral changes corresponding to 2A, B & C, respectively in each of the solutions on subtracting the absorption spectrum of the AuNPs solution.

Please cite this article as: N. Kumar et al., Label-free peptide nucleic acid biosensor for visual detection of multiple strains of influenza A virus suitable for field applications, Analytica Chimica Acta, https://doi.org/10.1016/j.aca.2019.09.060

way, the denaturation step was circumvented during the optimization of PNA visual assay by utilizing the high-affinity property of PNA and providing a low-ionic environment for hybridization to target RNA sequence which would otherwise have required a costly heating instrument.

3.2. Viral RNA quantification and analytical specificity assessment

The concentration-dependent spectral changes in each of the solutions (corresponding to that described in Fig. 2A, 2B and 2C) were more substantial on subtracting the absorption spectrum of the AuNPs solution (Fig. 2A', 2B′ and 2C′). These spectra facilitated in the selection of a convenient wavelength maxima (ratio of A_{640}/A_{520}) for the quantification of IAV RNA. Using this approach, the visual assay was adapted to quantify IAV RNA. Thus, the absorbance ratio of A_{640}/A_{520} was plotted against the varying $oligo_{comp}$ and IAV RNA concentrations which generated a linear correlation of $R^2 = 0.983$ and $R^2 = 0.974$, respectively (Fig. 2B and 2C). These R^2 values were comparable to a linear correlation of $R^2 = 0.992$ obtained with RT-qPCR experiment using the same viral RNA, and thus this assay could be used for viral RNA quantification with considerable accuracy.

Furthermore, the analytical specificity (inclusivity) of the visual assay was assessed against the OIE reference H1−H16 AIV subtypes. As shown in Fig. 1F, the assay demonstrated 100% specificity with no change in color against all the HA subtypes (H1−H16) of IAVs. Additionally, analytical specificity (exclusivity) of the visual assay confirmed that the designed PNA is highly specific to IAVs and did not cross-react with closely-related viral RNA (Newcastle Disease Virus, NDV), and distantly-related viral RNA (Enzootic Bovine Leukemia Virus, EBLV) and DNA (Ovine Herpesvirus-2, OvHV-2) viruses (Fig. 1E). Besides, the desalted PNA dissolved in HPLC grade water caused immediate aggregation of AuNPs while only HPLC grade water (blank control) could not. This confirmed that the specificity of aggregation of AuNPs is because of PNA and not because of other reagents such as cations present in the solution.

In our study, we did not include H17 and H18 IAVs that have recently been detected in bats as they are highly divergent compared to other HA subtypes (Fig. 1A). Furthermore, they are host-restricted (detected only in bats) and have not been associated with the poultry and public health risks until now.

3.3. Clinical utility of the visual assay

The most promising utility of developing any colorimetric assay reside on the '*lab to the field*' concept. To test this, we evaluated the performance of the visual assay for detection of IAVs on 419 cloacal samples of avian species and compared the results with RT-qPCR (Fig. 1G). The visual assay showed a high diagnostic specificity (96.46%, 95% CI = 93.8 to 98.2) and sensitivity (82.41%, 95% CI = 73.9 to 89.1) when RT−qPCR was used as reference test. The ROC curve analysis showed a very good distinguishing capacity (that differentiated IAV positive samples from the negative ones) of the visual assay (AUC = 0.894, 95% CI = 0.861 to 0.922, $p < 0.0001$) (Fig. 1H). Besides, the visual assay did not show any non-specific reactivity with RNA of many avian species cloacal samples, and thus the assay is suitable to screen IAVs in the complex fecal microbiota of many avian species. Furthermore, the strength of agreement between the visual assay and RT−qPCR results were calculated using kappa statistics and results showed a good correlation between the two assays (Weighted Kappa = 0.808, 95% CI = 0.743 to 0.874). Moreover, during an investigation of POSP (Post Operation Surveillance Plan) chicken samples received from farm holdings in Odisha (n = 5) and Jharkhand (n = 6) states of India recently in the month of March 2019; the visual assay (9/11) showed a very good correlation with RT-qPCR (10/11) for the detection of IAVs.

Significant advances have been made towards the development of biosensors for IAVs since the last few years. The biosensors developed so far allowed detection of IAVs of a specific HA subtype [28−32] or few HA subtypes [5,33], which restrict their applicability to selective HA subtypes. Other methods that allowed the detection of many HA subtypes require sophisticated instruments and are often restricted to the laboratory use [34]. Additionally, the efforts to utilize the potential of PNA to develop a visual assay for the detection of H1N1 [35] and amantadine drug-resistant IAV using fluorescein tagged PNA mediated RT−PCR [36] have been made. But, both of these assays either required costly instrumentation (thermocycler), tedious conjugation process or additional bio-reagent molecules.

To be more specific, the major limitations of IAVs specific biosensors developed so far are that they are either HA subtype-specific or require sophisticated instruments or both and most importantly, they have not been evaluated for their suitability on clinical samples. Unlike humans, the avian species are known to harbor H1−H16 subtypes of IAVs, thus, it becomes essential to develop an assay to detect all those HA subtypes. Hence, the present PNA biosensor was developed against the highly conserved M gene, to detect IAVs of all HA subtypes. The simple, fast, label-free, coupled with the capacity of visual detection in the absence of tedious conjugation procedure and expensive equipment, makes this assay more useful than other developed biosensors. Furthermore, the high diagnostic efficacy together with a very good concordance with RT−qPCR results on avian clinical samples proves this assay practical utility for use as a rapid point-of-care diagnostic for IAVs at field conditions.

4. Conclusions

We have demonstrated that the presence of complementary RNA sequence prevents the PNA induced unmodified AuNPs aggregation and this concept offers direct visual detection of IAVs RNA with high diagnostic specificity and sensitivity on avian clinical samples. The assay had a visual (naked eye) detection limit of 2.3 ng of direct viral RNA and showed high specificity to IAVs. Besides, the visual assay showed a very good correlation with RT−qPCR for the detection of IAVs. Thus, this assay could contribute to national−wide surveillance studies, especially at the herd level and implementing quick control measures at the early stages of an IAV epidemic. The simplicity and universality of this visual assay could also be applied to humans IAVs diagnostics.

Declaration of competing interest

The authors declare that they have no known competing financial interests or personal relationships that could have appeared to influence the work reported in this paper.

Credit authorship contribution statement

Naveen Kumar: Conceptualization, Methodology, Investigation, Writing - original draft, Supervision. **Sandeep Bhatia:** Investigation, Formal analysis, Project administration. **Atul Kumar Pateriya:** Visualization, Formal analysis, Data curation. **Richa Sood:** Resources, Writing - review & editing. **S. Nagarajan:** Resources, Writing - review & editing. **H.V. Murugkar:** Resources, Writing - review & editing. **Satish Kumar:** Conceptualization, Supervision, Writing - review & editing. **Praveen Singh:** Resources, Writing - review & editing. **Vijendra Pal Singh:** Funding acquisition, Project administration.

Please cite this article as: N. Kumar et al., Label-free peptide nucleic acid biosensor for visual detection of multiple strains of influenza A virus suitable for field applications, Analytica Chimica Acta, https://doi.org/10.1016/j.aca.2019.09.060

Declaration of competing interest

The authors declare that they have no known competing financial interests or personal relationships that could have appeared to influence the work reported in this paper.

Acknowledgments

The authors appreciatively recognize the Indian Council of Agricultural Research (ICAR), New Delhi, India and ICAR- National Institute of High Security Animal Diseases (ICAR-NIHSAD), Bhopal India for providing the infrastructure and facilities. The authors are grateful for financial support from the ICAR-NIHSAD (Project ID-IXX12891). The authors thank Professor James W. Schneider, Carnegie Mellon University, Pittsburgh, USA for sharing a detailed protocol for laboratory synthesis of PNA. The authors also thank Dr. Suresh Ghoke, College of Veterinary and Animal Sciences, Udgir, India for collecting different avian species cloacal samples from the Maharashtra state of India.

Appendix A. Supplementary data

Supplementary data to this article can be found online at https://doi.org/10.1016/j.aca.2019.09.060.

References

[1] R.G. Webster, W.J. Bean, O.T. Gorman, T.M. Chambers, Y. Kawaoka, Evolution and ecology of influenza A viruses, Microbiol. Rev. 56 (1992) 152–179.
[2] World Organization for Animal Health. http://www.oie.int/fileadmin/Home/eng/Animal_Health_in_the_World/docs/pdf/OIE_AI_situation_report/OIE_SituationReport_AI_August2018.pdf, 2018 assessed on May 10, 2019.
[3] World Health Organization. https://www.who.int/influenza/human_animal_interface/2019_04_09_tableH5N1.pdf?ua=1, 2019 assessed on May 10, 2019.
[4] Y.T. Tseng, C.H. Wang, C.P. Chang, G.B. Lee, Integrated microfluidic system for rapid detection of influenza H1N1 virus using a sandwich-based aptamer assay, Biosens. Bioelectron. 82 (2016) 105–111.
[5] R.Q. Zhang, S.L. Hong, C.Y. Wen, D.W. Pang, Z.L. Zhang, Rapid detection and subtyping of multiple influenza viruses on a microfluidic chip integrated with controllable micro-magnetic field, Biosens. Bioelectron. 100 (2018) 348–354.
[6] C. Chartrand, M.M. Leeflang, J. Minion, T. Brewer, M. Pai, Accuracy of rapid influenza diagnostic tests: a meta-analysis, Ann. Intern. Med. 156 (2012) 500–511.
[7] N.P. Pai, C. Vadnais, C. Denkinger, N. Engel, M. Pai, Point-of-care testing for infectious diseases: diversity, complexity, and barriers in low- and middle-income countries, PLoS Med. 9 (2012) e1001306.
[8] W. Zhao, M.A. Brook, Y. Li, Design of gold nanoparticle-based colorimetric biosensing assays, Chembiochem 9 (2008) 2363–2371.
[9] E.H. Lee, S.K. Lee, M.J. Kim, S.W. Lee, Simple and rapid detection of bisphenol A using a gold nanoparticle-based colorimetric aptasensor, Food Chem. 287 (2019) 205–213.
[10] J. Conde, J.M. de la Fuente, P.V. Baptista, RNA quantification using gold nanoprobes - application to cancer diagnostics, J. Nanobiotechnol. 8 (2010) 5.
[11] Y. Qi, L. Li, B. Li, Label-free detection of specific DNA sequence-telomere using unmodified gold nanoparticles as colorimetric probes, Spectrochim. Acta. A. Mol. Biomol. Spectrosc. 74 (2009) 127–131.
[12] W.A. El-Said, J.W. Choi, High selective spectroelectrochemical biosensor for HCV-RNA detection based on a specific peptide nucleic acid, Spectrochim. Acta. A. Mol. Biomol. Spectrosc. 217 (2019) 288–293.
[13] P. Jolly, M.R. Batistuti, A. Miodek, P. Zhurauski, M. Mulato, M.A. Lindsay, P. Estrela, Highly sensitive dual mode electrochemical platform for microRNA detection, Sci. Rep. 6 (2016) 36719.
[14] T.M. Godoy-Reyes, A.M. Costero, P. Gaviña, R. Martínez-Máñez, F. Sancenón, Colorimetric detection of normetanephrine, a pheochromocytoma biomarker, using bifunctionalised gold nanoparticles, Anal. Chim. Acta 1056 (2019) 146–152.
[15] P.E. Nielsen, M. Egholm, R.H. Berg, O. Buchardt, Sequence-selective recognition of DNA by strand displacement with a thymine-substituted polyamide, Science 254 (1991) 1497–1500.
[16] V. Demidov, M.D. Frank-Kamenetskii, M. Egholm, O. Buchardt, P.E. Nielsen, Sequence selective double strand DNA cleavage by peptide nucleic acid (PNA) targeting using nuclease S1, Nucleic Acids Res. 21 (1993) 2103–2107.
[17] R. Kanjanawarut, X. Su, Colorimetric detection of DNA using unmodified metallic nanoparticles and peptide nucleic acid probes, Anal. Chem. 81 (2009) 6122–6129.
[18] V.G. Joshi, K. Chindera, A.K. Singh, A.P. Sahoo, V.D. Dighe, D. Thakuria, A.K. Tiwari, S. Kumar, Rapid label-free visual assay for the detection and quantification of viral RNA using peptide nucleic acid (PNA) and gold nanoparticles (AuNPs), Anal. Chim. Acta 795 (2013) 1–7.
[19] J.P. Vernille, L.C. Kovell, J.W. Schneider, Peptide nucleic acid (PNA) amphiphiles: synthesis, self-assembly, and duplex stability, Bioconjug. Chem. 15 (2004) 1314–1321.
[20] K. Zabetakis, W.E. Ghann, S. Kumar, M.C. Daniel, Effect of high gold salt concentrations on the size and polydispersity of gold nanoparticles prepared by an extended Turkevich–Frens method, Gold Bull. 45 (2012) 203–211.
[21] T. Kawada, Receiver operating characteristic curve analysis, sensitivity comparison and individual difference, Clin. Radiol. 67 (2012) 940.
[22] J.R. Landis, G.G. Koch, The measurement of observer agreement for categorical data, Biometrics 33 (1977) 159–174.
[23] X. Su, R. Kanjanawarut, Control of metal nanoparticles aggregation and dispersion by PNA and PNA-DNA complexes, and its application for colorimetric DNA detection, ACS Nano 3 (2009) 2751–2759.
[24] A. Gourishankar, S. Shukla, K.N. Ganesh, M. Sastry, Isothermal titration calorimetry studies on the binding of DNA bases and PNA base monomers to gold nanoparticles, J. Am. Chem. Soc. 126 (2004) 13186–13187.
[25] P. Eaton, P. Quaresma, C. Soares, C. Neves, M.P. de Almeida, E. Pereira, P. West, A direct comparison of experimental methods to measure dimensions of synthetic nanoparticles, Ultramicroscopy 182 (2017) 179–190.
[26] N. Dias, C. Sénamaud-Beaufort, E.E. Forestier, C. Auvin, C. Hélène, T. Ester Saison-Behmoaras, RNA hairpin invasion and ribosome elongation arrest by mixed base PNA oligomer, J. Mol. Biol. 320 (2002) 489–501.
[27] H. Orum, P.E. Nielsen, M. Jørgensen, C. Larsson, C. Stanley, T. Koch, Sequence-specific purification of nucleic acids by PNA-controlled hybrid selection, Biotechniques 19 (1995) 472–480.
[28] J. Bhardwaj, A. Sharma, J. Jang, Vertical flow-based paper immunosensor for rapid electrochemical and colorimetric detection of influenza virus using a different pore size sample pad, Biosens. Bioelectron. 126 (2019) 36–43.
[29] Y. Horiguchi, T. Goda, A. Matsumoto, H. Takeuchi, S. Yamaoka, Y. Miyahara, Direct and label-free influenza virus detection based on multisite binding to sialic acid receptors, Biosens. Bioelectron. 92 (2017) 234–240.
[30] A. Hushegyi, D. Pihíková, T. Bertok, V. Adam, R. Kizek, J. Tkac, Ultrasensitive detection of influenza viruses with a glycan-based impedimetric biosensor, Biosens. Bioelectron. 79 (2016) 644–649.
[31] S.H. Kim, J. Lee, B.H. Lee, C.S. Song, M.B. Gu, Specific detection of avian influenza H5N2 whole virus particles on lateral flow strips using a pair of sandwich-type aptamers, Biosens. Bioelectron. 134 (2019) 123–129.
[32] M. Sayhi, O. Ouerghi, K. Belgacem, M. Arbi, Y. Tepeli, A. Ghram, Ü. Anik, L. Österlund, D. Laouini, M.F. Diouani, Electrochemical detection of influenza virus H9N2 based on both immunomagnetic extraction and gold catalysis using an immobilization-free screen printed carbon microelectrode, Biosens. Bioelectron. 107 (2018) 170–177.
[33] C.H. Wang, C.P. Chang, G.B. Lee, Integrated microfluidic device using a single universal aptamer to detect multiple types of influenza viruses, Biosens. Bioelectron. 86 (2016) 247–254.
[34] D. Nidzworski, P. Pranszke, M. Grudniewska, E. Król, B. Gromadzka, Universal biosensor for detection of influenza virus, Biosens. Bioelectron. 59 (2014) 239–242.
[35] K. Kaihatsu, S. Sawada, S. Nakamura, T. Nakaya, T. Yasunaga, N. Kato, Sequence-specific and visual identification of the influenza virus NS gene by azobenzene-tethered bis-peptide nucleic acid, PLoS One 8 (2013) e64017.
[36] K.C. Tsao, C.C. Chiou, T.L. Chen, C.G. Huang, E.F. Hsieh, S.R. Shih, Detection of low copies of drug-resistant influenza viral gene by a single-tube reaction using peptide nucleic acid as both PCR clamp and sensor probe, J. Microbiol. Immunol. Infect. 47 (2014) 254–256.